

MULTIAXIAL FATIGUE AND DEFECT ASSESSMENT OF TRUCK STABILIZERS

S. Beretta¹, H. Desimone², A. Poli³

^{1,2}Politecnico di Milano, ^{2,3}Tenaris Dalmine

^{1,2}Via La Masa 34, 20158 MILANO (Italy), ^{2,3}Piazza Caduti 1, 24044 DALMINE (Italy)
stefano.beretta@polimi.it;hernan.desimone@polimi.it;apoli@tenaris.com

Abstract

Automotive stabilizers are safety components and it is therefore important to assess their fatigue behaviour in terms of real load conditions as well as material strength. For the second point, a detrimental effect in the fatigue limit of high strength steels is given by the defects present in the component, coming from the material (as microinclusions, microvoids, etc) or for the process (as, for example, handling marks), in other words, it is vital to analyse the risk of failure in presence of inhomogeneities in order to improve component reliability. In particular stabilizers are subjected to multiaxial fatigue. For this reason, in this paper, starting from FEM analysis in order to obtain the stresses in the component, a defect assessment is carried out considering round and planar surface defects in terms of its SIFs. Results are then analysed in terms of maximum SIF against the ΔK_{th} for short cracks, which were obtained experimentally.

Introduction

The automotive industry is facing a severe conflict concerning the vehicle weight. If for one hand the target is to obtain a drastic CO₂ reduction, for the other hand the tendency is to enhance either the safety as the performance characteristic of the vehicle. In this context, the novel high-strength steel (HSS) grades represent a cost efficient method to overcome this conflict (Pimminger and Pichler, [1]). For this reason, the application of HSS in vehicles started for several percent in the beginning of the 90^{ies} and are at present over the 50% in some vehicles.

This increasing demand on HSS gives rise to a series of 'new' topics to be addressed, specially regarding its application to fatigue loads. In fact, when HSS are subjected to fatigue loads, as in the case of a stabilizer, the defects that are present in it (as for example inclusions, microvoids or surface imperfections) could originate crack stable growth starting from them and finally, they could derive in the whole component failure. For this reason, in order to assess the fatigue behaviour of a HSS vehicle component, it is crucial to analyse the possible propagation of cracks from the material defects; reliability of the component can then be eventually achieved with improvements in component design and process.

In this paper, focus on surface defects will be made, since it has been shown that the most detrimental position for defects is when they become 'tangent' to the surface, thus being similar to surface defects (Murakami, [2]).

Stress Analysis

In order to introduce the problem, here the FEM analysis of the stresses is reported, showing also the more loaded zones, at least in terms of Von Mises stresses.

FEM Model

The FEM model has been developed to predict the stress field in the stabilizer under prescribed load conditions. Fig. 1 shows a general view of the whole model used for the analysis. In particular the stabilizer, developed for a truck, has the following dimensions: the tube has an outside diameter of $D=65\text{mm}$ and a thickness $t=10.5\text{mm}$, being $b=440\text{mm}$ and $L=1050\text{mm}$. The load F has been taken as the one usually considered for high cycle fatigue life acceptance test.

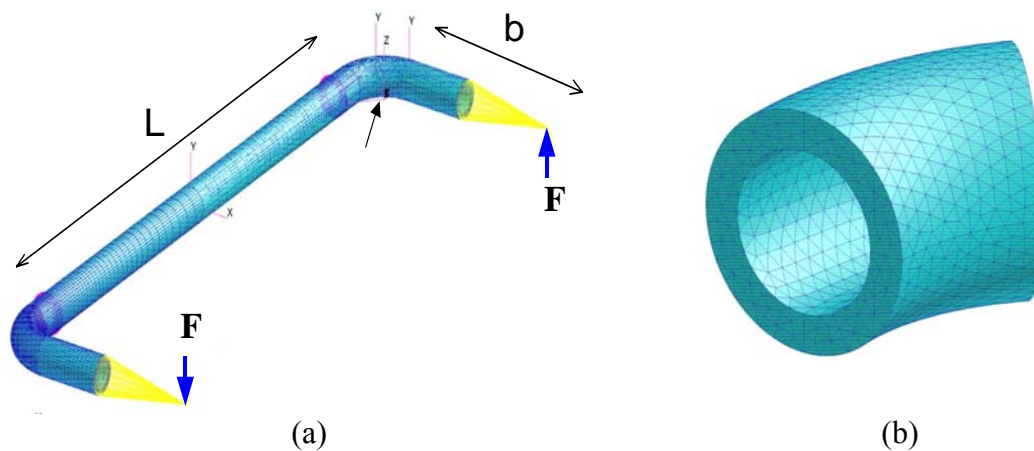


FIGURE 1. The FEM model: a) general view; b) a detail of the mesh along the curve.

The arms of the bar have been modelled with a solid tubular shape only in the part close to the curved one: the other part have been modelled with a series of beams because it was not important to know the stress field in these parts. For the curved part tetrahedral elements with 10 nodes each were used, while in the straight parts, such as the arms and the torsion bar, wedge elements with 15 nodes each were utilised. The aim of this type of mesh is to obtain a precise map of stresses in the curved part with a low number of nodes and elements in the model. According to this, it was decided to adopt a mesh along the thickness in the curved part and an extruded mesh in the others. The result is a model with about 140000 nodes.

FEM Results

Fig. 2 shows the results in terms of normalised (to the maximum) Von Mises stress. At first sight (Fig. 2a) it is evident that the relevant areas, in terms of high stresses, are localised along the curves. In Fig. 2b the stresses in the external surface of the outer part of the curve are reported, and it is possible to observe that the regions of high stresses are reduced in comparison with the inner part. Fig. 2c and 2d show the stress field in the internal surface of the curved part: as it can be observed the Von Mises stresses are lower here than in the external surfaces. Zones with more relevant stresses are symmetric respect the middle plane of the stabilizer, approximately at 45° (Fig. 2a).

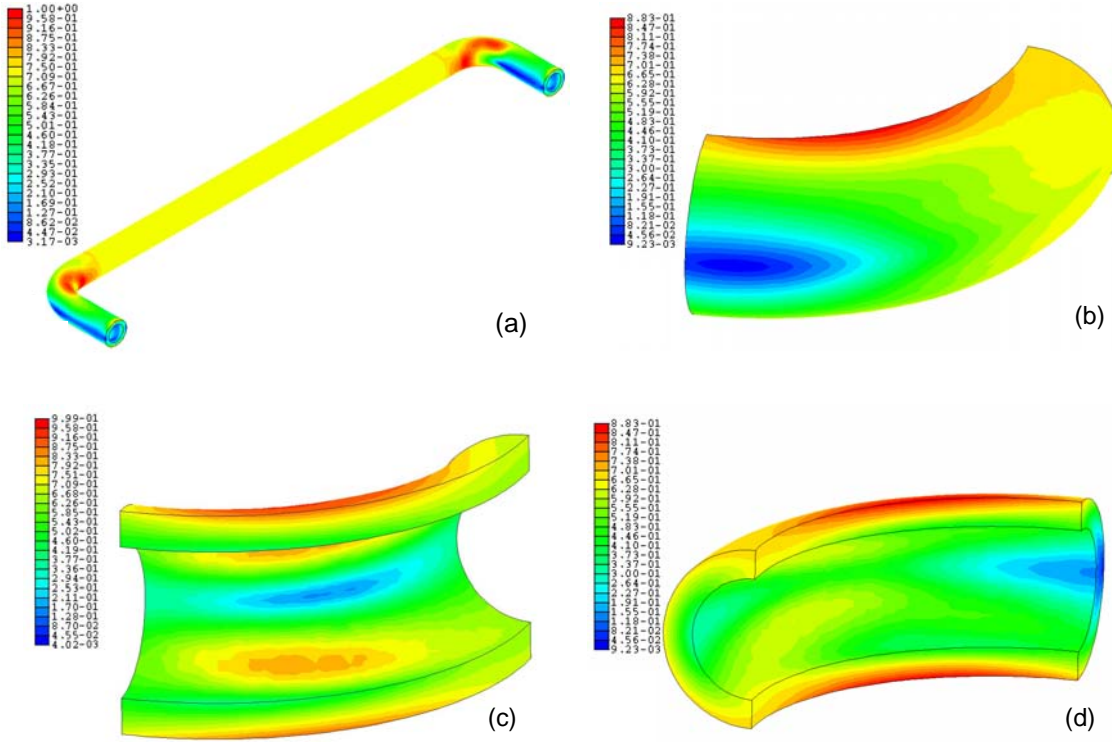


FIGURE 2. Von Mises normalised stresses a) general view; b) outer radius and external surface; c) inner radius and internal surface d) outer radius and: internal surface

Method - Defect Criticality

For a steel with medium or high level of hardness, the fatigue limit is usually determined by the presence of defects (Murakami, [2]). Experimental evidences have shown that near the fatigue limit non-propagating cracks usually exist at the tip of defects: in this way fatigue limit corresponds to the threshold conditions of these cracks [2]. For this reason, in order to asses the fatigue behaviour of a stabilizer, the propagation from surface defects should be taken into account. In this paper, two kind of surface defects on a stabilizer will be analysed: a round defect and a planar flaw in longitudinal direction (Fig. 3).

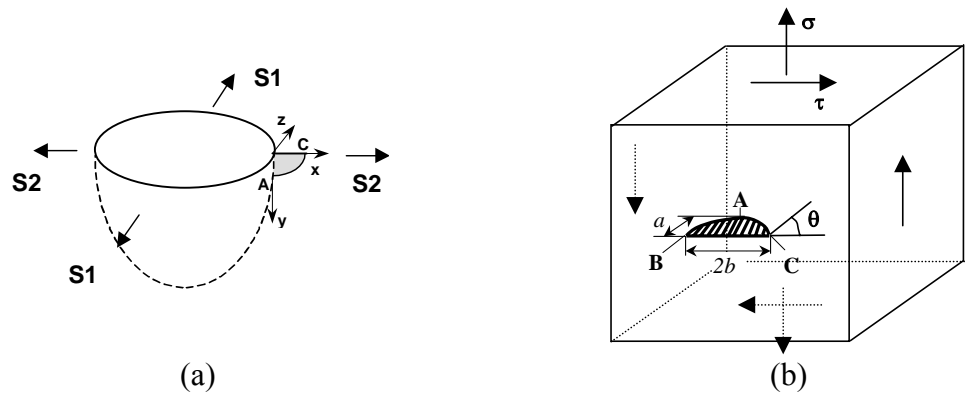


FIGURE 3. Defects considered in the present work: a) Round; b) Planar.

Round defect

Considering the presence of a round defect subjected to a simple uniaxial stress, the SIF for the non-propagating cracks at the tip of the defect can be calculated with Murakami's formula [2]:

$$\Delta K = 0.65 \cdot \Delta \sigma \cdot \sqrt{\pi \cdot \sqrt{\text{area}}} \quad (1)$$

being $\sqrt{\text{area}}$ the square root of the projected defect surface. Under a biaxial in-phase state of stress the SIF can be derived from a uniaxial stress by knowing the principal stresses S_1 and S_2 , using the weight function method (Beretta and Murakami [3]):

$$\frac{K_{I,\text{tens}}}{K_{I,\text{biaxial}}} = 1 + 0.1804 \cdot S_2/S_1 + 0.0329 \cdot (S_2/S_1)^2 \quad (2)$$

Being K_I the SIF due only to S_1 and $K_{I,\text{biaxial}}$, the SIF due to S_1 and S_2 . Then, according to Murakami's theory, the fatigue limit is assumed to be determinate by the threshold condition for the non-propagating cracks at the defect tip. In other words, the fatigue failure of the component (or the criticality of a given defect) can be determined in terms of the propagation index (PI), defined as:

$$PI = \frac{\Delta K_{\text{biaxial}}}{\Delta K_{th}} \geq 1 \quad (3)$$

where it is assumed that the fatigue will occur if PI is bigger than one.

Planar Defect

In the case of planar defect, the fatigue torsional limit is determined by the non-propagating condition of Mode I branch cracks at the initial crack (Murakami *et al.* [4]). Therefore, in order to assess the criticality of a planar defect, in conditions of mixed-mode loads, the maximum K_I in terms of a possible branch from the original defect must be evaluated.

A longitudinal planar defect is subjected to mode II and III, due to the shear stresses along the plane where the defect is included, and to mode I, due to the circumferential stress. The K_I stress intensity factor for the original configuration (please avoid confusion with the K_I for the prospective branch) can be computed using the Newman and Raju [5] solution and mode II and mode III stress intensity factors, caused by shear, can be computed from Kassir and Sih [6], who obtained the solution of the stress intensity factor under a remote uniform shear stress.

In particular, for tips B and C, where K_{III} is zero, the Erdogan and Sih criterion [7] derives in the following equation:

$$K_{\theta_{\max}} = \cos \frac{\theta_0}{2} \left(K_I \cos^2 \frac{\theta_0}{2} - \frac{3}{2} K_{II} \sin \theta_0 \right) \quad (4)$$

being θ_0 the angle between the branching plane and the plane where the original crack is included (see Fig. 4a). For the A tip, where K_{II} is zero and K_{III} reaches its maximum value, the branch tends to occur in a 'tilt' plane (Figure 4b), given place in this way to the so-called 'twist' crack (Pook, [8]). The K_I corresponding to this plane is given by:

$$K_{\theta_{\max}} = \frac{K_I (1 + 2\nu) + \left[K_I^2 (1 - 2\nu)^2 + 4K_{III}^2 \right]^{1/2}}{2} \quad (5)$$

As for the round defect, the Propagation Index could now be defined in the way

$$PI = \frac{\Delta K_{\theta_{\max}}}{\Delta K_{th}} \quad (6)$$

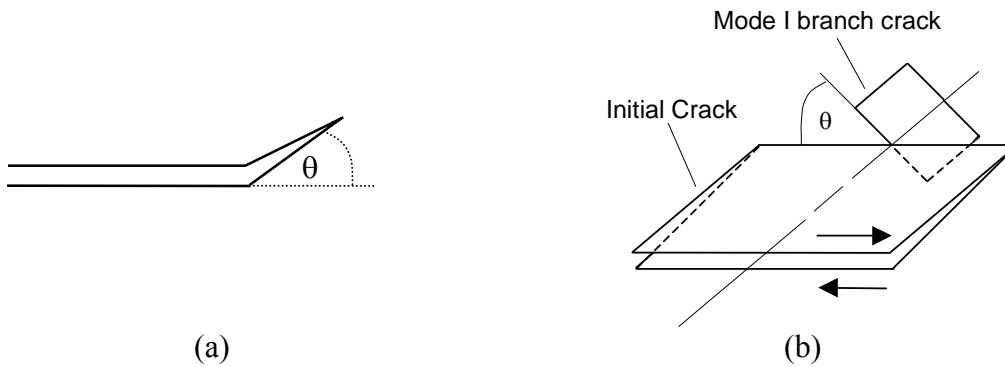
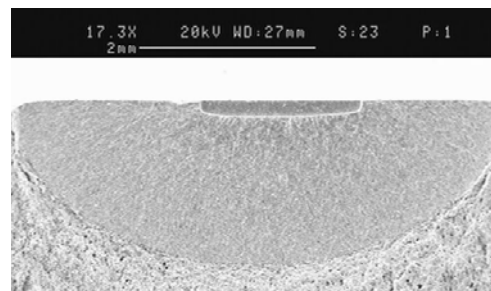
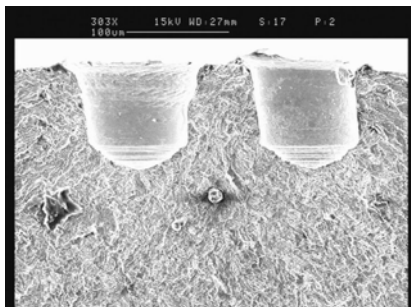


FIGURE 4. The angle for the prospective plane of propagation: a) tips B and C; b) tip A.

Fatigue experiments

Material Properties

The examined material is Dal512®, a quenched and tempered microalloyed steel produced by Tenaris. Mechanical properties of the examined steel are: ultimate tensile strength 1350 MPa, 0.2% yield stress 1230 MPa, cyclic yield strength 850 MPa, elongation at fracture 6%.



(a)

(b)

FIGURE 5. SEM analysis of a) the micro-holes; b) narrow defects obtained by EDM

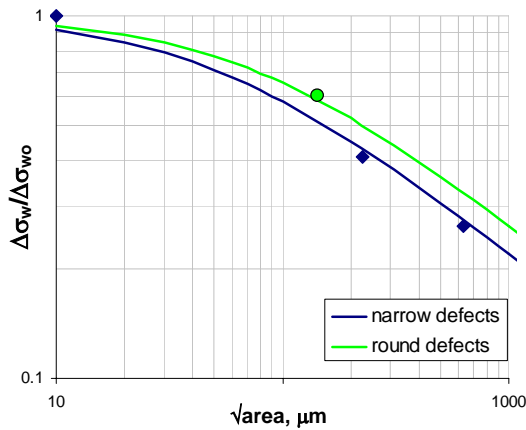
Thresholds for short cracks

Fatigue threshold for short cracks were determined by fatigue limit tests on smooth and micro-notched specimens. Micro-holes were used for obtaining defects in the range of 100-200 μm of $\sqrt{\text{area}}$ (Fig.5a). Narrow slits obtained by electro-discharge machining (EDM) were used for defects in the range of 250-650 μm of $\sqrt{\text{area}}$ (Fig.5b). In particular fatigue tests were carried out for obtaining a complete description of the so-called Kitagawa and Takahashi [9] diagram at $R=-1$. Results are reported in Fig. 6a.

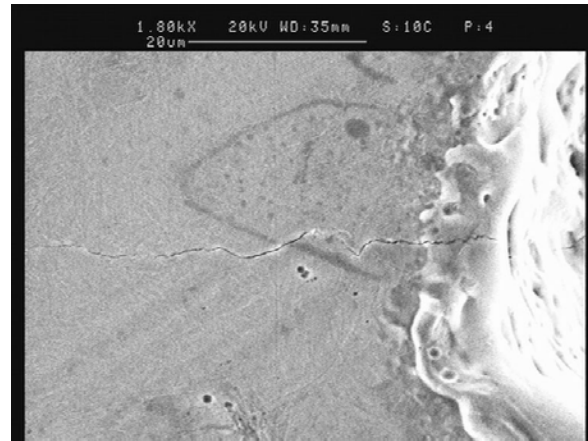
Fig. 6b shows a non-propagating crack emanating from two micro-holes, for a run-out specimen. Similar results have been obtained on the whole run-out specimens. This fact confirms that fatigue limit corresponds to the threshold condition of these non-propagating cracks and in this way it is possible to use the Murakami's equation (1) in order to transform fatigue limit data into threshold data, arriving to [10]:

$$\Delta K_{\text{th}} = \Delta K_{\text{th,LC}} \cdot \sqrt{\frac{\sqrt{\text{area}}}{\sqrt{\text{area}} + \sqrt{\text{area}_0}}} \quad (7)$$

where $\Delta K_{\text{th,LC}}$ is the threshold for long cracks, $\sqrt{\text{area}}$ is the crack (or defect) size and the term $\sqrt{\text{area}_0}$ represents the so-called “fictitious crack size”. This is the threshold to be compared with the SIF coming from round and planar defects. The resulting relationship between fatigue limit and defect size is also shown in Fig. 6a.



(a)



(b)

FIGURE 6. a) The Kitagawa diagram for Dal512® material; b) Non-propagating crack at the tip of an EDM micro-notch.

Results

The method is here presented by analysing two defects: a round subsurface cavity with a $\sqrt{\text{area}}$ of 0.3mm and a planar one of the same $\sqrt{\text{area}}$, with a depth of 0.1mm and a length of 1mm. The planar defect has an aspect relation b/a equal to 5. Results are shown in Figures 7 (round defect) and 7 (planar one) in terms of its Propagation Index.

At least two important conclusions could be deduced from these results. The first one is that, for the same $\sqrt{\text{area}}$, the planar defect is as detrimental as the round one, in the internal surface, although the depth of the planar defect is smaller compared with the round one (compare Fig 7a with Fig 8a).

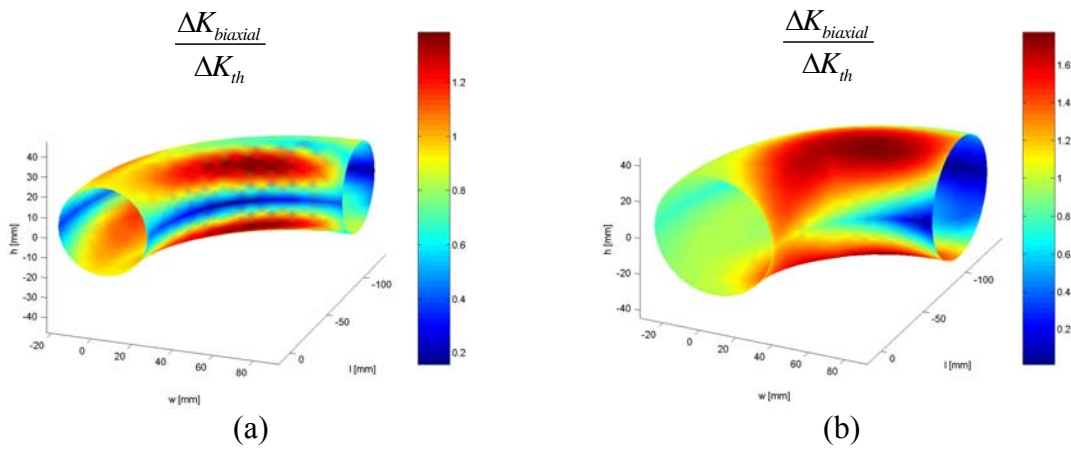


FIGURE 7. Propagation index for *round* defects: a) internal surface; b) external surface

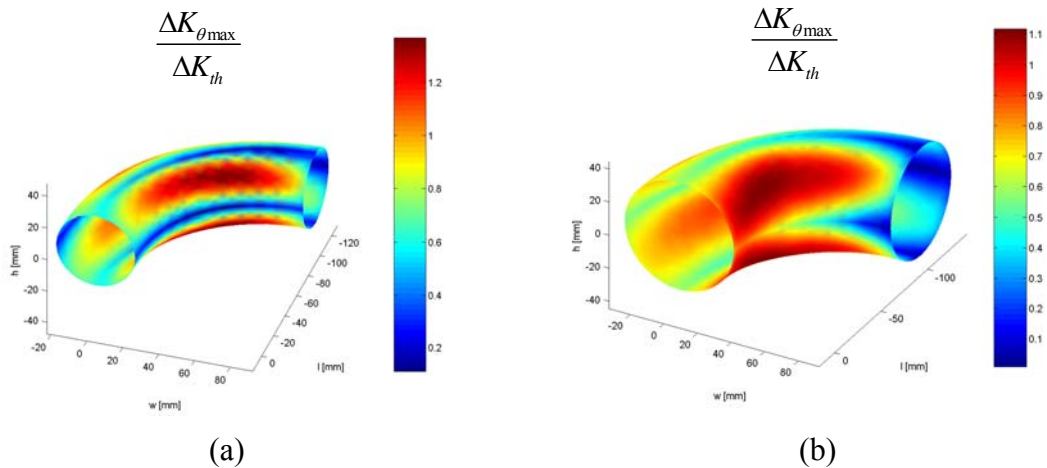


FIGURE 8. Propagation index for *planar* defects: a) internal surface; b) external surface

The second conclusion is that planar defects are more detrimental in the internal surface than in the external one (Fig 8a versus Fig 8b). This is due to the circumferential stresses.

In fact, the planar defects here are assumed to be longitudinal due to manufacturing process. For this reason, the planar defects are subjected to circumferential stresses, which give origin to K_I . As the circumferential stresses are high in the internal side, the Propagation Index for the planar defects reflects this condition.

It is important to add, that here also an unique value of ΔK_{th} in all the thickness was assumed, but actually in the external surface, due to shot peening, the thresholds are higher than in the internal side. In other words, defects in the internal size are likely to be more dangerous. It is also worth remarking that the region of high severity index shown in Figures 10 and 11 is in fully agreement with the failure origin found in the fatigue test of these components.

Conclusions

A technique including experimental and theoretical part has been proposed in order to assess the fatigue behaviour of vehicles components, focusing in the importance of the defects. The method here proposed has been applied with success to stabilizers, but can be extended almost straightforward to other kind of automotive components subjected to fatigue. The proposed approach gives also to the designer an important information in order to optimise geometry and weight of the component as well as the final superficial treatment on the component (as the mentioned shot peening process).

Acknowledgements

The authors want to thank to Mr Magnus Baarman and Mrs Kaisa Niskala of Styria Group for their collaboration to the present research.

References

1. M. Pimminger, A. Pichler, *Proceedings of the 4th European Oxygen Steelmaking Conference*, Graz, May 2003.
2. Murakami Y, *Metal Fatigue*, Elsevier, Oxford, 2003.
3. Beretta S, Murakami Y, *Fat. Fract. Engng. Mater. Struct.*, vol. **23**, 97-104, 2000.
4. Murakami Y, Takahashi K, Toyama K, *Proceedings International Conference on Fatigue Crack Paths*, Parma, September 2003.
5. Newman JC, Raju IS, *Engng. Frac. Mech.*, vol. **15**, 185-192, 1981.
6. Kassir MK, Sih GC, *Trans. ASME, E. J. Appl. Mech*, vol **33**, 601-611, 1966.
7. Erdogan F, Sih GC, *Journal of Basic Engineering*, 519-527, 1963.
8. Pook LP, *Crack Paths*, WitPress, Southampton, UK, 2002 .

9. Kitagawa H, Takahashi S, *2nd International Conference on Mechanical Behaviour of Materials*, Boston, Mass, Aug. 1976, pp. 627-631.
10. Beretta S. *Proceedings of the 14th European Conf. on Fracture*, Krakow, Poland, September 2002.